



# Topological zero modes and Dirac points protected by spatial symmetry and chiral symmetry

Mikito Koshino,<sup>1</sup> Takahiro Morimoto,<sup>2</sup> and Masatoshi Sato<sup>3</sup>

<sup>1</sup>*Department of Physics, Tohoku University, Sendai 980-8578, Japan*

<sup>2</sup>*Condensed Matter Theory Laboratory, RIKEN, Wako, Saitama 351-0198, Japan*

<sup>3</sup>*Department of Applied Physics, Nagoya University, Nagoya 464-8603, Japan*

(Received 11 June 2014; published 22 September 2014)

We explore a new class of topologically stable zero-energy modes which are protected by coexisting chiral and spatial symmetries. If a chiral-symmetric Hamiltonian has an additional spatial symmetry such as reflection, inversion, and rotation, the Hamiltonian can be separated into independent chiral-symmetric subsystems by the eigenvalue of the space symmetry operator. Each subsystem supports chiral zero-energy modes when a topological index assigned to the block is nonzero. By applying the argument to Bloch electron systems, we detect band touching at symmetric points in the Brillouin zone. In particular, we show that Weyl nodes appearing in honeycomb lattice (e.g., graphene) and in half-flux square lattice are protected by threefold and twofold rotation symmetry, respectively. We also present several examples of Dirac semimetal with isolated band-touching points in three-dimensional  $k$  space, which are protected by combined symmetry of rotation and reflection. The zero-mode protection by spatial symmetry is distinct from that by the conventional winding number. We demonstrate that symmetry-protected band touching points emerge even though the winding number is zero. Finally, we identify relevant topological charges assigned to the gapless points.

DOI: [10.1103/PhysRevB.90.115207](https://doi.org/10.1103/PhysRevB.90.115207)

PACS number(s): 71.20.-b, 73.22.-f, 73.61.-r

## I. INTRODUCTION

The chiral symmetry is one of the fundamental symmetries used to classify the topological states of matter [1–3]. The symmetry relates positive and negative parts in the energy spectrum, and a nontrivial topological nature is linked to a singular property at zero energy. The chiral symmetry is also called sublattice symmetry, because the bases are divided into two sublattices with different eigenvalues of the chiral operator  $\Gamma = +1$  and  $-1$ , and the Hamiltonian has no matrix elements inside the same sublattice group. The difference between the number of sublattices of  $\Gamma = +1$  and  $-1$  is a topological index which cannot change continuously. A nontrivial index indicates the existence of topologically protected zero-energy modes. If the chiral Hamiltonian is defined in a phase space, on the other hand, we have another topological invariant defined by a winding number (Berry phase) for a closed path [1,4–7]. Nonzero winding number is also a source of topological objects such as band touching points and zero-energy boundary modes.

A chiral-symmetric system frequently comes with other material-dependent spatial symmetry such as reflection, rotation, and inversion. Recent progress in the study on the topological phase has revealed that the existence of the spatial symmetry enriches the topological structure of the system [8–17]. The spatial symmetry often stabilizes the band touching points which are otherwise unstable. For example, the reflection symmetry defines topological crystalline insulators with mirror Chern numbers [11], where an even number of stable Dirac cones exist on the surface [18–20], which are generally unstable in the ordinary topological insulators [21,22]. We have a similar situation in Weyl semimetals in three dimensions [23–25]. Weyl semimetals have stable gapless low-energy excitations that are described by a  $2 \times 2$  Weyl Hamiltonian, and the spectrum is generally gapped out when two Weyl nodes with opposite topological charges merge at the same  $k$  point. In the presence of additional spatial symmetry, however, we may have Dirac semimetals with gapless low-energy excitations described by a  $4 \times 4$  Dirac

Hamiltonian [26–29], and it has been confirmed experimentally in  $\text{Cd}_3\text{As}_2$  and  $\text{Na}_3\text{Bi}$  [30–32]. Generally, a zero-energy mode or gapless mode in a band structure is topologically stable when it is realized as an intersect of constraints given by the secular equation in momentum space [33,34]. Sophisticated topological arguments based on the K theory enable us to classify possible intersects systematically as topological obstructions, predicting gapless modes consistent with the spatial symmetries [35–37].

In this paper, we find a new class of zero-energy modes protected by the coexistence of chiral symmetry and spatial symmetry. If a chiral-symmetric system has an additional symmetry such as reflection, inversion, and rotation, the Hamiltonian can be block diagonalized into the eigenspaces of the symmetry operation, and each individual sector is viewed as an independent chiral-symmetric system. There we can define a topological index as the difference between the numbers of sublattices, and a nonzero index indicates the existence of chiral zero-energy modes in that sector. As a result, the number of total zero-energy modes are generally larger than in the absence of the spatial symmetry.

If we apply the argument to Bloch electron systems, we can detect the existence of zero-energy band touching at symmetric points in the Brillouin zone. This argument predicts the existence of gapless points solely from the symmetry, without even specifying the detail of the Hamiltonian. In particular, we show that the Dirac nodes appearing in a two-dimensional (2D) honeycomb lattice (e.g., graphene) and in a half-flux square lattice are protected by threefold ( $C_3$ ) and twofold ( $C_2$ ) rotation symmetry, respectively. We also present examples of Dirac semimetal with isolated band-touching points in three-dimensional (3D)  $k$  space, which are protected by rotation and reflection symmetry. The zero-mode protection by spatial symmetry is distinct from that by the conventional winding number, and we actually demonstrate in several concrete models that symmetry-protected band touching points emerge even though the winding number is zero.

In the last part of the paper, we list and classify all independent topological invariants associated with a given Dirac point under chiral and spatial symmetries. They consist of winding numbers and topological indices (sublattice number difference) of the subsectors of the spatial symmetry operator, with the redundant degrees of freedom removed. If the spatial symmetry is of order two (i.e., two times of operation is proportional to identity, like reflection and inversion), we can use the K theory with Clifford algebra to identify how many quantum numbers are needed to label all topologically distinct phases [35–37]. We explicitly show that a set of independent winding numbers and topological indices serves as complete topological charges found in the K theory.

The paper is organized as follows. In Sec. II, we present a general formulation for zero modes protected by the coexistence of chiral symmetry and spatial symmetry. We then discuss protection of the Dirac points in  $C_3$  symmetric crystals in Sec. III and that in  $C_2$  symmetric crystals in Sec. IV, respectively. We also argue line-node protection by additional reflection symmetry in Sec. V. Several examples of 3D Dirac semimetal are studied in Sec. VI. In Sec. VII, we identify independent topological charges assigned to gapless points and clarify the relation to the classification theory using Clifford algebra. Finally, we present a brief conclusion in Sec. VIII.

## II. GENERAL ARGUMENTS

We first present a general argument for zero modes protected by a space symmetry in a chiral-symmetric system. We consider a Hamiltonian  $H$ , satisfying

$$[H, A] = 0, \quad (1)$$

$$\{H, \Gamma\} = 0, \quad (2)$$

where  $\Gamma$  is the chiral operator and  $A$  is the operator describing the spatial symmetry of the system. We also assume

$$[\Gamma, A] = 0, \quad (3)$$

i.e., the sublattices belonging to  $\Gamma = 1$  and  $-1$  are not interchanged by  $A$ .

Since  $[H, A] = [\Gamma, A] = 0$ , the matrices  $H$ ,  $\Gamma$ , and  $A$  are simultaneously block diagonalized into subspaces labeled by the eigenvalues of  $A$  as

$$\begin{aligned} H &= \begin{pmatrix} H_{a_1} & & & \\ & H_{a_2} & & \\ & & H_{a_3} & \\ & & & \ddots \end{pmatrix}, \\ \Gamma &= \begin{pmatrix} \Gamma_{a_1} & & & \\ & \Gamma_{a_2} & & \\ & & \Gamma_{a_3} & \\ & & & \ddots \end{pmatrix}, \\ A &= \begin{pmatrix} a_1 & & & \\ & a_2 & & \\ & & a_3 & \\ & & & \ddots \end{pmatrix}, \end{aligned} \quad (4)$$

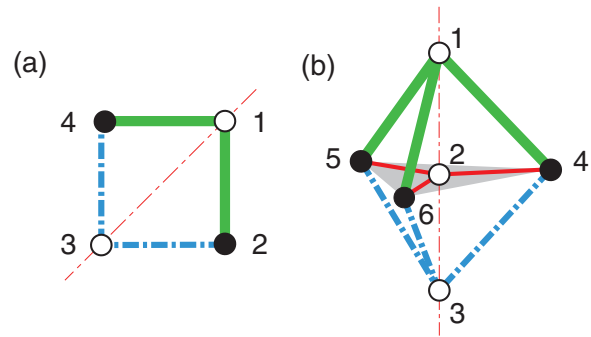


FIG. 1. (Color online) (a) Four-site model with reflection symmetry on a diagonal axis. (b) Six-site model with threefold rotation symmetry.

where  $a_1, a_2, \dots$  are the eigenvalues of  $A$ . Since Eq. (2) requires  $\{H_{a_i}, \Gamma_{a_i}\} = 0$  for all the sectors, each eigenspace possesses chiral symmetry independently. Then we can define the topological index for each sector as

$$v_{a_i} = \text{tr } \Gamma_{a_i}. \quad (5)$$

The index  $v_{a_i}$  is equal to the difference of the chiral zero modes of the Hamiltonian  $H_{a_i}$ ,

$$v_{a_i} = N_{a_i}^+ - N_{a_i}^-, \quad (6)$$

where  $N_{a_i}^\pm$  are numbers of chiral zero modes satisfying

$$\begin{aligned} H_{a_i} |u_{a_i}^\pm\rangle &= 0, \\ \Gamma_{a_i} |u_{a_i}^\pm\rangle &= \pm |u_{a_i}^\pm\rangle. \end{aligned} \quad (7)$$

Equation (6) guarantees that there are at least  $|v_{a_i}|$  zero modes in each sector and therefore at least  $\sum_i |v_{a_i}|$  zero modes in the total system.

On the other hand, the topological index for the total Hamiltonian is given by the summation over all the subindices as

$$v_0 = \sum_i v_{a_i}, \quad (8)$$

which in itself guarantees  $|v_0|$  zero modes. Since  $\sum_i |v_{a_i}| \geq |\sum_i v_{a_i}|$ , we can generally have more zero modes in the presence of additional symmetry  $A$  than in its absence.

As the simplest example, let us consider a four-site square lattice as illustrated in Fig. 1(a). We assume that the system is invariant under the reflection  $R$  with respect to a diagonal line connecting the sites 1 and 3. We also assume that the lattice is bipartite, i.e., matrix elements only exist between white circles (sites 1 and 3) and black circles (2 and 4). Then the system is chiral symmetric under the chiral operator  $\Gamma$  defined by

$$\Gamma |i\rangle = \begin{cases} +|i\rangle & (i = 1, 3) \\ -|i\rangle & (i = 2, 4), \end{cases} \quad (9)$$

where  $|i\rangle$  is the state localized at the site  $i$ . The operators  $\Gamma$  and  $R$  satisfies  $[\Gamma, R] = 0$  since the black and white circles are not interchanged by  $R$ . The topological index of the total system,  $v_0 = \text{tr } \Gamma$ , is obviously zero, since there are even numbers of white and black circles.

Since  $[H, R] = [\Gamma, R] = 0$ ,  $H$  and  $\Gamma$  are block diagonalized into subspaces each labeled by the eigenvalues of  $R$ . Each subspace is spanned by

$$\begin{aligned} R = \text{even: } & |1\rangle, |3\rangle, \frac{1}{\sqrt{2}}(|2\rangle + |4\rangle) \\ R = \text{odd: } & \frac{1}{\sqrt{2}}(|2\rangle - |4\rangle). \end{aligned} \quad (10)$$

The topological indices of each subblock is written as

$$\begin{aligned} \nu_{\text{even}} &= \text{tr } \Gamma_{\text{even}} = +1 \\ \nu_{\text{odd}} &= \text{tr } \Gamma_{\text{odd}} = -1, \end{aligned} \quad (11)$$

so the number of protected zero modes is  $|\nu_{\text{even}}| + |\nu_{\text{odd}}| = 2$ . By breaking the reflection symmetry, the number of zero modes is actually reduced to  $|\nu_0| = 0$ ,

We may consider another example having  $C_3$  rotation symmetry. Here we introduce a six-site lattice model shown in Fig. 1(b), where the sites 1, 2, and 3 (white circles) are located at the  $z$  axis, and sites 4, 5, and 6 (black circles) are arranged in a triangle around the origin. The system is invariant under the  $C_3$  rotation with respect to  $z$  axis, where the sites 1, 2, and 3 are fixed while 4, 5, and 6 are circularly permuted. The lattice is bipartite so the Hamiltonian is chiral symmetric under  $\Gamma$  defined by

$$\Gamma|i\rangle = \begin{cases} +|i\rangle & (i = 1, 2, 3) \\ -|i\rangle & (i = 4, 5, 6). \end{cases} \quad (12)$$

Since  $[H, C_3] = [\Gamma, C_3] = 0$ ,  $H$  and  $\Gamma$  are block diagonalized into subspaces spanned by

$$\begin{aligned} C_3 = 1: & |1\rangle, |2\rangle, |3\rangle, \frac{1}{\sqrt{3}}(|4\rangle + |5\rangle + |6\rangle), \\ C_3 = \omega: & \frac{1}{\sqrt{3}}(|4\rangle + \omega^2|5\rangle + \omega|6\rangle), \\ C_3 = \omega^2: & \frac{1}{\sqrt{3}}(|4\rangle + \omega|5\rangle + \omega^2|6\rangle), \end{aligned} \quad (13)$$

where  $\omega = \exp(2\pi i/3)$ . The topological indices of three subspace become

$$(\nu_1, \nu_\omega, \nu_{\omega^2}) = (2, -1, -1). \quad (14)$$

The number of protected zero modes is  $|\nu_1| + |\nu_\omega| + |\nu_{\omega^2}| = 4$ , while we have only  $|\nu_0| = 0$  zero modes in the absence of  $C_3$  symmetry.

### III. DIRAC POINTS IN HONEYCOMB LATTICE

Now let us extend the argument in the previous section to Bloch electron systems. In this section, we discuss the topological protection of the Dirac points in 2D systems in the presence of threefold rotation symmetry. For the Bloch Hamiltonian  $H(\mathbf{k}) = e^{-i\mathbf{k}\cdot\mathbf{r}} H e^{i\mathbf{k}\cdot\mathbf{r}}$ , the chiral symmetry and the threefold rotation symmetry are given by unitary operators

$\Gamma$  and  $C_3$  that satisfy

$$\begin{aligned} \Gamma H(\mathbf{k}) \Gamma^{-1} &= -H(\mathbf{k}), \\ C_3 H(\mathbf{k}) C_3^{-1} &= H(R_3(\mathbf{k})), \end{aligned} \quad (15)$$

where  $R_3(\mathbf{k})$  denotes a momentum rotated by  $120^\circ$  around the origin. We assume the commutation relation of chiral operator and threefold rotation,

$$[\Gamma, C_3] = 0. \quad (16)$$

Let us consider the high symmetry point in the Brillouin zone that is invariant under an action of threefold rotation;  $R_3(\mathbf{k}^0) = \mathbf{k}^0$ . There Eq. (15) reduces to

$$\begin{aligned} \{H(\mathbf{k}^0), \Gamma\} &= 0, \\ [H(\mathbf{k}^0), C_3] &= 0, \end{aligned} \quad (17)$$

and we can apply the previous argument to  $H = H(\mathbf{k}^0)$ . We simultaneously block-diagonalize  $H$ ,  $\Gamma$ , and  $C_3$  into three sectors each labeled by an eigenvalue of  $C_3$  and define a topological index for each eigenspace as

$$\nu_a = \text{tr } \Gamma_a, \quad (18)$$

with  $a = 1, \omega, \omega^2$ . If  $\sum_a |\nu_a|$  is nonzero, it requires an existence of chiral zero modes of  $H(\mathbf{k}^0)$ , i.e., we have a topologically stable gap closing at  $\mathbf{k}^0$  protected by the chiral symmetry and  $C_3$  symmetry.

Graphene is the simplest example of the band touching protected by  $C_3$  symmetry. Let us consider a tight-binding honeycomb lattice with nearest-neighbor hopping, as shown in Fig. 2(a). The unit cell is composed of nonequivalent A and B sublattices. The Hamiltonian is chiral symmetric in that A is only connected to B, and the system is obviously invariant under threefold rotation  $C_3$ .  $C_3$  commutes with  $\Gamma$  because the rotation does not interchange A and B sublattices. The Brillouin zone corners  $K$  and  $K'$ , shown in Fig. 2(b), are fixed in  $C_3$  rotation so we can apply the above argument to these points. We define the Bloch wave basis as

$$|X\rangle = \frac{1}{\sqrt{N}} \sum_{\mathbf{R}_X} e^{i\mathbf{k}\cdot\mathbf{R}_X} |\mathbf{R}_X\rangle \quad (X = A, B), \quad (19)$$

where  $\mathbf{k}$  is the Bloch wave vector ( $K$  or  $K'$ ),  $|\mathbf{R}_X\rangle$  is the atomic state at the position  $\mathbf{R}_X$ , and  $N$  is the number of unit cells in the whole system. In the basis of  $\{|A\rangle, |B\rangle\}$ , the chiral operator is written as

$$\Gamma = \begin{pmatrix} 1 & \\ & -1 \end{pmatrix}. \quad (20)$$

If we set the rotation center at A site, the rotation  $C_3$  is written as

$$C_3 = \begin{pmatrix} 1 & \\ & \omega \end{pmatrix} \text{ for } K, \begin{pmatrix} 1 & \\ & \omega^2 \end{pmatrix} \text{ for } K'. \quad (21)$$

This is actually derived by considering the change of the Bloch factor in the rotation [Fig. 2(a) for the  $K$  point]. Therefore, the topological indices are obtained as

$$(\nu_1, \nu_\omega, \nu_{\omega^2}) = \begin{cases} (1, -1, 0) & \text{for } K, \\ (1, 0, -1) & \text{for } K'. \end{cases} \quad (22)$$

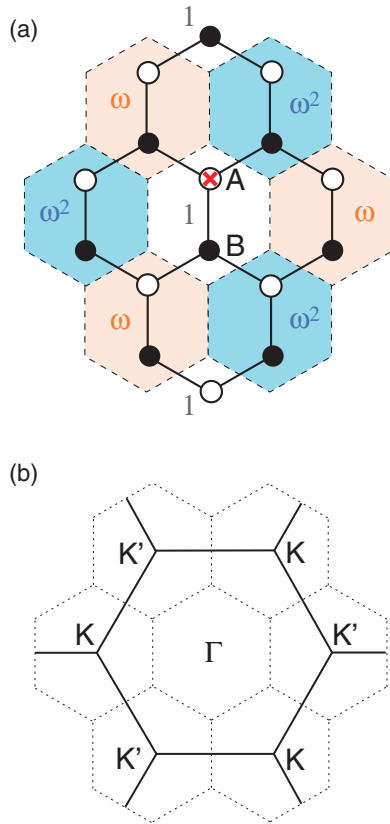


FIG. 2. (Color online) (a) Honeycomb lattice with nearest-neighbor hopping. The unit cell is indicated by a dashed hexagon, and shading represents the Bloch phase factor  $\exp(i\mathbf{K} \cdot \mathbf{r}) = 1, \omega, \omega^2$  at the  $K$  point. (b) Brillouin zone for the honeycomb lattice. Dotted, small hexagon is the reduced Brillouin zone corresponding to the  $\sqrt{3} \times \sqrt{3}$  superlattice in Figs. 3(a) and 3(b).

This requires two zero modes at each of  $K$  and  $K'$ , which are nothing but the gapless Dirac nodes [38,39]. Note that the band touching is deduced purely from the symmetry in the Bloch bases, without specifying detailed Hamiltonian matrix.

In this particular case, the gaplessness at  $K$  and  $K'$  can also be concluded from the nontrivial winding number  $\nu_W = \pm 1$  around  $K$  and  $K'$ , respectively. (For details of the winding number, see Sec. VII A.) However, these two different arguments are not generally equivalent, and actually  $C_3$ -protected band touching may occur even though the winding number is zero, as shown in the following. Let us consider a tight-binding honeycomb lattice with  $\sqrt{3} \times \sqrt{3}$  superlattice distortion as shown in Figs. 3(a) and 3(b), where the hopping amplitudes for thin and thick bonds are differentiated. In accordance with the enlarged unit cell, the Brillouin zone is folded as shown in Fig. 2(b), where the original  $K$ ,  $K'$ , and  $\Gamma$  points are folded onto the new  $\Gamma$  point. Then  $\nu_W$  around the  $\Gamma$  point is contributed from  $\pm 1$  around the original  $K$  and  $K'$ , respectively, so we have trivial winding number  $\nu_W = 0$  as a whole. However, we can show that the Dirac point remains ungapped even in the presence of the superlattice distortion, when the system keeps a certain threefold rotation symmetry. We consider two different types of rotations as

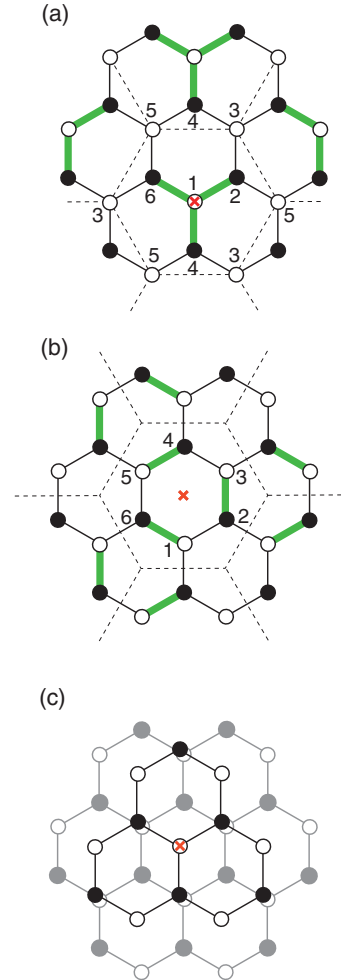


FIG. 3. (Color online) [(a) and (b)]  $\sqrt{3} \times \sqrt{3}$  superlattice unit cell of graphene, with possible lattice distortion under (a)  $C_3$  and (b)  $C'_3$  symmetry. The center of the rotation is indicated by the X. (c) Structure of graphite, where black and gray layers stack alternatively.

follows:

$$C_3: 120^\circ \text{ rotation around A site.}$$

$$C'_3: 120^\circ \text{ rotation around the center of hexagon.}$$

Figures 3(a) and 3(b) are examples of the lattice distortion under  $C_3$  and  $C'_3$  symmetry, respectively. The latter case, Fig. 3(b), is the so-called Kekulé distortion.

The unit cell contains six atoms as depicted in Fig. 3. On the basis of  $\{|1\rangle, |2\rangle, \dots, |6\rangle\}$ , the chiral operator is given by

$$\Gamma = \begin{pmatrix} 1 & & & & & \\ & -1 & & & & \\ & & 1 & & & \\ & & & -1 & & \\ & & & & 1 & \\ & & & & & -1 \end{pmatrix}, \quad (23)$$

and the threefold rotation at the  $\Gamma$  point is represented by

$$C_3 = \begin{pmatrix} 1 & & & \\ & 1 & & \\ & & 1 & \\ & & & 1 \end{pmatrix}, \quad (24)$$

$$C'_3 = \begin{pmatrix} & & & 1 \\ & & 1 & \\ & 1 & & \\ 1 & & & \end{pmatrix}.$$

The topological indices of three sectors are given by

$$(\nu_1, \nu_\omega, \nu_{\omega^2}) = \begin{cases} (2, -1, -1) & \text{for } C_3, \\ (0, 0, 0) & \text{for } C'_3. \end{cases} \quad (25)$$

Nontrivial topological indices in  $C_3$  symmetry require four zero modes, indicating that the two Dirac points are protected. In  $C'_3$  symmetry, on the other hand, the topological indices are all zero and the energy band is gapped out. The situation of  $C_3$  symmetry closely resembles the six-site model in the previous section, where the fixed points in the rotation (the sites 1, 3, and 5) all contribute to the sector of  $C_3 = 1$ , leading to an imbalance in the topological indices among the three sectors. In contrast, all the sites are circularly interchanged in  $C'_3$  rotation, resulting in  $\nu_1 = \nu_\omega = \nu_{\omega^2} = \nu_0/3 = 0$ .

We can derive the same conclusion alternatively by starting from a  $4 \times 4$  low-energy effective Hamiltonian,

$$H = k_x \sigma_x \tau_z + k_y \sigma_y, \quad (26)$$

where Pauli matrices  $\sigma$  and  $\tau$  span the sublattice ( $A, B$ ) and the valley ( $K, K'$ ) degrees of freedom, respectively. The dimension of the matrix is smaller than the previous argument ( $6 \times 6$ ) because we exclude the two high-energy bases from the original  $\Gamma$  point, which do not contribute to the topological indices. The chiral operator is given by

$$\Gamma = \sigma_z = \begin{pmatrix} 1 & & & \\ & -1 & & \\ & & 1 & \\ & & & -1 \end{pmatrix}. \quad (27)$$

The matrices for  $C_3$  and  $C'_3$  are derived by considering the Bloch factor in the original lattice model as

$$C_3 = \begin{pmatrix} 1 & & & \\ & \omega & & \\ & & 1 & \\ & & & \omega^2 \end{pmatrix} = \exp \left[ -\frac{\pi i}{3} (\sigma_z - 1) \tau_z \right]. \quad (28)$$

$$C'_3 = \begin{pmatrix} \omega & & & \\ & \omega^2 & & \\ & & \omega^2 & \\ & & & \omega \end{pmatrix} = \exp \left[ \frac{2\pi i}{3} \sigma_z \tau_z \right], \quad (29)$$

The topological indices are immediately shown to be equivalent to Eq. (25).

Possible mass terms under the chiral symmetry which gap out the Hamiltonian of Eq. (26) anticommute with both  $H$  and  $\Gamma$ . In the present case we have two such terms,

$$\delta H = m_x \sigma_x \tau_x + m_y \sigma_x \tau_y. \quad (30)$$

Since  $\delta H$  commutes with  $C'_3$  but not with  $C_3$ , these terms can exist only in  $C'_3$  symmetry. This exactly corresponds to the fact that the Dirac point is not protected in  $C'_3$  symmetry. Actually, Kekulé distortions depicted in Fig. 3(b) give rise to mass terms  $\delta H$  and gap out the Dirac point.

The argument can be directly extended to a 3D crystal with  $C_3$  symmetry. There the band touching point forms a line node on the  $C_3$  symmetric axis in the 3D Brillouin zone. A typical example of this is a bulk graphite, where graphene layers are stacked in an alternative way between black and gray layers as in Fig. 3(c). When we consider the threefold rotation symmetry around the center of the hexagon of a gray layer (the  $X$  in the figure), the topological indices are obtained as

$$(\nu_1, \nu_\omega, \nu_{\omega^2}) = \begin{cases} (1, 0, -1) & \text{for } K, \\ (1, -1, 0) & \text{for } K'. \end{cases} \quad (31)$$

which guarantees two line nodes at  $K$  and  $K'$  parallel to the  $k_z$  direction. A real graphite is not exactly chiral symmetric because of some minor hopping amplitudes between black and black (white and white) atoms. As a result, the line node slightly disperses in the  $k_z$  axis, giving electron and hole pockets at zero energy [40].

#### IV. DIRAC POINTS IN HALF-FLUX SQUARE LATTICE

The square lattice with half magnetic flux penetrating a unit cell is another well-known example having gapless Dirac nodes [41]. The band touching in this system can also be explained by a similar argument, in terms of the chiral symmetry and  $C_2$  rotation symmetry. We consider a lattice Hamiltonian illustrated in Fig. 4(a). The unit cell is represented by a dashed diamond including sites 1 and 2 inside. The hopping integral along the horizontal bond is all identical to  $t_x$ , while the vertical hopping depends on the direction and is given by  $it_y$  for the hopping in the direction of the arrow. An electron always acquires the factor  $-1$  when moving around any single plaquette, so it is equivalent to the half magnetic flux penetrating a unit cell.

The system is  $C_2$ -rotation symmetric with respect to an arbitrary atomic site, and the rotation commutes with the chiral operator since it does not interchange the sublattices. In the reciprocal space [Fig. 4(c)], the points  $K : (\pi/(2a), \pi/(2a))$  and  $K' : (-\pi/(2a), \pi/(2a))$  are both invariant in the  $C_2$  rotation, and we apply the general argument to these points. In the basis of  $\{|1\rangle, |2\rangle\}$ , the chiral operator is written as

$$\Gamma = \begin{pmatrix} 1 & \\ & -1 \end{pmatrix}, \quad (32)$$

and the  $C_2$  rotation with respect to site 1 is

$$C_2 = \begin{pmatrix} 1 & \\ & -1 \end{pmatrix} \quad \text{for } K \text{ and } K'. \quad (33)$$

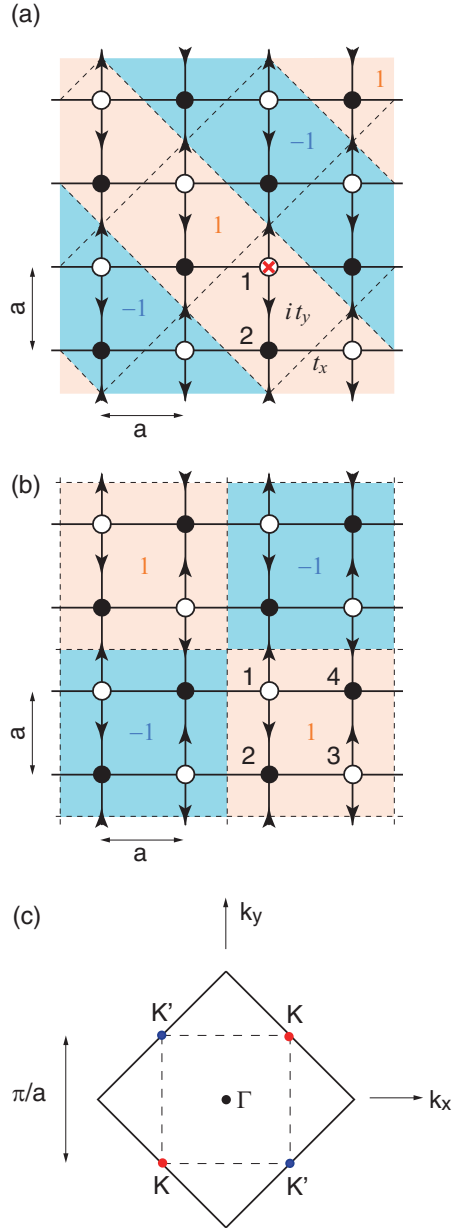


FIG. 4. (Color online) (a) Square lattice with a half magnetic flux penetrating unit cell. The unit cell is indicated by a dashed diamond, and shading represents the Bloch phase factor for the  $K$  point. (b) The same system with a double unit cell. (c) Brillouin zone for the single unit cell in (a). The dashed square is the reduced Brillouin zone corresponding to the double unit cell in (b).

Thus the topological indices are

$$(\nu_{\text{even}}, \nu_{\text{odd}}) = (1, -1) \text{ for } K \text{ and } K', \quad (34)$$

where even and odd specify the eigenvalue of  $C_2$  rotation  $+1$  and  $-1$ , respectively. As a result, we have two zero modes at each of  $K$  and  $K'$ , corresponding to the band touching points.

Similarly to the honeycomb lattice in the previous section, we may consider the stability of the Dirac points under possible lattice distortions for the double unit cell shown in Fig. 4(b). In the reciprocal space,  $K$  and  $K'$  merge at the same corner point and the total winding number becomes zero. We consider two

types of rotations as follows:

$C_2$ :  $180^\circ$  rotation around site 1.

$C'_2$ :  $180^\circ$  rotation around the center of square.

In the basis of  $\{|1\rangle, |2\rangle, |3\rangle, |4\rangle\}$ , the chiral operator is given by

$$\Gamma = \begin{pmatrix} 1 & & & \\ & -1 & & \\ & & 1 & \\ & & & -1 \end{pmatrix}, \quad (35)$$

and the  $180^\circ$  rotation at the merged  $k$  point is represented by

$$C_2 = \begin{pmatrix} 1 & & & \\ & -1 & & \\ & & 1 & \\ & & & -1 \end{pmatrix}, \quad (36)$$

$$C'_2 = \begin{pmatrix} & & 1 & \\ & & & 1 \\ 1 & & & \\ & 1 & & \end{pmatrix}.$$

The topological indices are given by

$$(\nu_{\text{even}}, \nu_{\text{odd}}) = \begin{cases} (2, -2) & \text{for } C_2, \\ (0, 0) & \text{for } C'_2, \end{cases} \quad (37)$$

so the two Dirac points are protected in  $C_2$  symmetry but not in  $C'_2$  symmetry.

The same conclusion can be reproduced in terms of the low-energy effective Hamiltonian, in a manner similar to that in Sec. III. The effective Hamiltonian and the chiral symmetry are given by

$$H = k_x \sigma_x \tau_z + k_y \sigma_y, \quad \Gamma = \sigma_z, \quad (38)$$

with  $\sigma$  and  $\tau$  spanning the sublattice ( $|1\rangle, |2\rangle$ ) and the valley ( $K, K'$ ) of the  $\pi$ -flux lattice. By taking into account the Bloch factor properly, the twofold rotations  $C_2, C'_2$  are identified as

$$C_2 = \sigma_z, \quad C'_2 = \sigma_z \tau_z. \quad (39)$$

Since the effective Hamiltonian and the chiral symmetry take the same forms as those in the honeycomb lattice case, possible mass terms consistent with the chiral symmetry are given by the same Eq. (30). Those mass terms are apparently inconsistent with the  $C_2$  symmetry above but consistent with the  $C'_2$  symmetry. Thus, between the two types of rotations, only the  $C_2$  symmetry does not allow these mass terms, keeping the Dirac points gapless.

## V. LINE NODE PROTECTED BY REFLECTION SYMMETRY

As another example, we consider a 2D lattice with reflection symmetry. In this case, the band touching is protected on the diagonal lines in the 2D Brillouin zone and forms line nodes. We take a lattice model as illustrated in Fig. 5, where the unit cell is composed of four sublattices from 1 to 4, and the structure is reflection symmetric with respect to the diagonal lines. In the basis of  $\{|1\rangle, |2\rangle, |3\rangle, |4\rangle\}$ , the chiral operator is

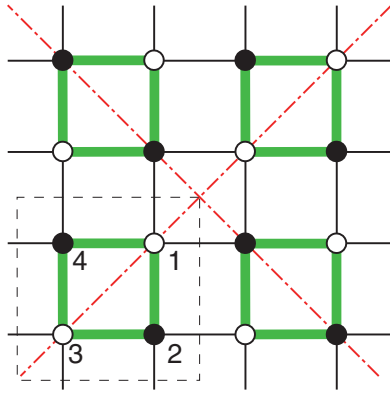


FIG. 5. (Color online) Square lattice model with the reflection symmetry. Dashed square indicates a unit cell and the diagonal line is a symmetry axis.

given by

$$\Gamma = \begin{pmatrix} 1 & & & \\ & -1 & & \\ & & 1 & \\ & & & -1 \end{pmatrix}. \quad (40)$$

We consider the reflection  $R$  with respect to the line connecting the sites 1 and 3. The fixed  $k$  points under  $R$  are given by  $\mathbf{k}_0 = (k, k)$  with arbitrary  $k$ . There the matrix for  $R$  is written as

$$R = \begin{pmatrix} 1 & & & \\ & & & 1 \\ & & 1 & \\ & 1 & & \end{pmatrix}. \quad (41)$$

The situation is exactly the same as the four-site model in Sec. II, and the topological indices of two sectors become

$$(v_{\text{even}}, v_{\text{odd}}) = (1, -1). \quad (42)$$

Since  $|v_{\text{even}}| + |v_{\text{odd}}| = 2$ , two energy bands are touching along the diagonal axis in the Brillouin zone. The same argument applies to the reflection for another diagonal line, giving a line node at  $(k, -k)$ .

## VI. DIRAC POINTS IN THREE DIMENSIONS

Here we present some examples of 3D Dirac system, where the band touching occurs at isolated  $k$  points in 3D Brillouin zone. First, we consider a stack of honeycomb lattices with staggered interlayer coupling as illustrated in Fig. 6(a). Here the honeycomb layers are vertically stacked at interlayer spacing  $c$ , and the vertical hopping between the neighboring layers is given by  $t$  and  $-t$  for  $A$  and  $B$  sublattices, respectively. The smallest unit cell of this system is given by  $A$  and  $B$  on a single layer, while we here take a double unit cell including  $A1, B1, A2, B2$ , so the Hamiltonian becomes chiral symmetric by grouping  $(A1, B2)$  into  $\Gamma = +1$  and  $(B1, A2)$  into  $-1$ . The effective Hamiltonian is given by

$$H = k_x \sigma_x \tau_z + k_y \sigma_y + 2t \cos(k_z c) \sigma_z \rho_x, \quad (43)$$

where Pauli matrices  $\sigma$  and  $\rho$  span the sublattice  $(A, B)$  and the layer  $(1, 2)$  degrees of freedom, respectively, and  $\tau_z = \pm 1$  is the valley indices for  $K$  and  $K'$ , respectively. Equation (43)

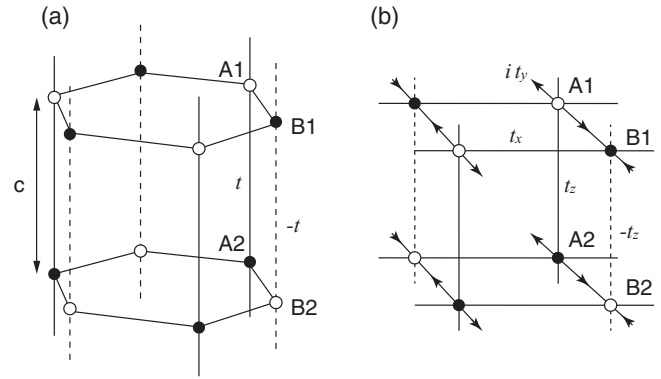


FIG. 6. (a) Stacked honeycomb lattices with staggered interlayer coupling. (b) Cubic lattice with a half magnetic flux penetrating every square plaquette.

has a gapless node at  $\mathbf{k}^0 = (0, 0, \pi/(2c))$ , and two Dirac cones are degenerate at this point. Note that the lattice period in the  $z$  direction is  $2c$ , so  $-\mathbf{k}^0$  is equivalent to  $\mathbf{k}^0$ .

The gapless point at  $\mathbf{k}^0$  can be concluded from the symmetry argument without the band calculation. The chiral operator is given by  $\Gamma = \rho_z \sigma_z$ , which obviously anticommutes with the Hamiltonian. We consider  $C_3$  rotation with respect to the  $A1$ - $A2$  axis and the reflection  $R_z$  with respect to the  $A1$ - $B1$  layer. The Hamiltonian is invariant and the point  $\mathbf{k}^0$  is fixed under these operations. Now we consider a combined operation  $C_3 R_z$  at  $\mathbf{k}_0$ . Since  $(C_3 R_z)^6 = 1$ , the eigenvalues of  $C_3 R_z$  are  $\pm 1, \pm \omega$ , or  $\pm \omega^2$ . For the  $K$  valley, for example, the matrix of  $C_3 R_z$  in a basis of  $\{|A1\rangle, |B1\rangle, |A2\rangle, |B2\rangle\}$  becomes

$$C_3 R_z = \text{diag}(1, \omega, -1, -\omega), \quad (44)$$

i.e., the four sublattices are classified to all different sectors. The number of zero modes is  $\sum_a |v_a| = 4$ , which guarantees the existence of Dirac nodes (doubly degenerate Weyl nodes). The argument equally applies to more general cases where the vertical hopping at the  $A$  and  $B$  sites is given by  $t_A$  and  $t_B$  (instead of  $t$  and  $-t$ ), respectively.

We can create another example of 3D Dirac nodes by stacking the 2D  $\pi$ -flux lattice in Sec. IV with staggered interlayer coupling. The model is illustrated in Fig. 6(b), where  $\pi$ -flux lattices are vertically stacked with the hopping  $t_z$  and  $-t_z$  for the  $A$  and  $B$  sublattices, respectively. The system can be viewed as a cubic lattice with a half magnetic flux threading every single square plaquette. We take a unit cell composed of  $A1, B1, A2$ , and  $B2$ , and group  $(A1, B2)$  into  $\Gamma = +1$  and  $(B1, A2)$  into  $-1$  so the Hamiltonian becomes chiral symmetric. We have band touching at  $K : \pi/(2a)(1, 1, 1)$  and  $K' : \pi/(2a)(-1, 1, 1)$ , and the effective Hamiltonian near these point nodes is given by

$$H = k_x \sigma_x \tau_z + k_y \sigma_y - k_z \sigma_z \rho_x, \quad (45)$$

where Pauli matrices  $\sigma$  and  $\rho$  span the sublattice  $(A, B)$  and the layer  $(1, 2)$  degrees of freedom, respectively, and  $\tau_z = \pm 1$  is the valley indices for  $K$  and  $K'$ , respectively. The chiral operator is given by  $\Gamma = \rho_z \sigma_z$ .

The gapless point in this model is protected by the inversion symmetry  $P = C_2 R_z$ . If we consider the inversion  $P$  with respect to  $A1$  site,  $K$  and  $K'$  are both invariant, and we can

TABLE I. Topological charges of the Dirac points in the presence of chiral symmetry and spatial symmetry. We assume that symmetry operators commute with each other.

Dimensions	Symmetries	Charges
2D	$\Gamma, C_N$	$\mathbb{Z}^N$
3D	$\Gamma, C_3 R_z$	$\mathbb{Z}^3$
3D	$\Gamma, C_2, R_z$	$\mathbb{Z}^2$
3D	$\Gamma, P$	$\mathbb{Z}$

write  $P = \rho_z \sigma_z$  at these points. We then find  $(\nu_{\text{even}}, \nu_{\text{odd}}) = (2, -2)$ , and thus we have doubly degenerate Weyl nodes at each of  $K$  and  $K'$ .

## VII. CLASSIFICATION OF TOPOLOGICAL CHARGES

In this section, we present general arguments to classify the Dirac points in the presence of chiral symmetry and spatial symmetry. We identify relevant topological numbers associated with protection of the Dirac points. In Table I, we summarize our results on topological charges of the Dirac points obtained in this section.

### A. Class AIII+ $C_N$ in 2D

First, let us study 2D Dirac points in class AIII systems (possessing chiral symmetry  $\Gamma$ ) with additional  $N$ -fold rotation symmetry  $C_N$ . We assume the commutation relation  $[\Gamma, C_N] = 0$ ; the Dirac points in Sec. III and Sec. IV are of this class.

In the presence of the chiral symmetry, we can define a winding number for a circle  $S^1$  surrounding the Dirac point in the Brillouin zone [1]. When the circle  $S^1$  is parameterized by  $\theta \in [0, 2\pi)$ , the winding number is given by

$$\nu_W = \frac{1}{4\pi i} \oint_{S^1} d\theta \text{tr}[\Gamma H^{-1}(\mathbf{k}(\theta)) \partial_\theta H(\mathbf{k}(\theta))]. \quad (46)$$

Here the Hamiltonian is gapped on  $S^1$  so the inverse  $H^{-1}(\mathbf{k}(\theta))$  is well defined. In a basis where the chiral operator  $\Gamma$  is diagonal,

$$\Gamma = \begin{pmatrix} 1 & 0 \\ 0 & -1 \end{pmatrix}, \quad (47)$$

the Hamiltonian takes an off-diagonal form written as

$$H(\mathbf{k}) = \begin{pmatrix} 0 & D^\dagger(\mathbf{k}) \\ D(\mathbf{k}) & 0 \end{pmatrix}. \quad (48)$$

Here  $\text{tr} \Gamma$  must be zero (i.e.,  $D$  is a square matrix), since otherwise zero-energy states remain independently of  $\mathbf{k}$ . The winding number is then recast into

$$\nu_W = \frac{1}{2\pi} \text{Im} \left[ \oint_{S^1} d\theta \partial_\theta \ln \det D(\mathbf{k}(\theta)) \right]. \quad (49)$$

It is evident that  $\nu_W$  is quantized to an integer since the phase change of  $\det D(\mathbf{k}(\theta))$  around  $S^1$  must be a multiple of  $2\pi$ .

As we have seen in Sec. II, by making use of rotation symmetry  $C_N$ , we can further define topological indices  $\nu_{a_n}$  [ $a_n = \exp(2\pi n i/N)$ ,  $n = 0, 1, 2, \dots, N-1$ ] by Eq. (6), for the Dirac points at  $C_N$ -symmetric  $k$  points. Since we have

$\sum_n \nu_{a_n} = \text{tr} \Gamma = 0$ , the number of independent indices are  $N-1$ . Thus the topological charges assigned to the Dirac point are

$$(\nu_W, \nu_{a_1}, \dots, \nu_{a_{N-1}}) \in \mathbb{Z}^N. \quad (50)$$

The Dirac points with nontrivial topological charges are stable against perturbations preserving chiral and rotation symmetry. In Sec. III and Sec. IV, we show examples of the Dirac points protected by nontrivial indices  $\nu_{a_i}$ , while the winding number  $\nu_W$  is trivial. In this sense, these are canonical examples of gapless points whose stability is not captured only by local symmetry (chiral symmetry) but originates from spatial symmetry.

For twofold rotation  $C_2$ , we can also use the K theory and Clifford algebra to classify gapless points [3,6,35–37,42–44]. In this case, the symmetry operators  $C_2$  and  $\Gamma$  can be considered an element of complex Clifford algebra  $Cl_n = \{e_1, \dots, e_n\}$  with generators  $e_1, \dots, e_n$  satisfying the anticommutation relation

$$\{e_i, e_j\} = 2\delta_{ij}. \quad (51)$$

Hence, the powerful representation theory of the Clifford algebra is available in the classification. Below we show that the approach with Clifford algebra provides the same topological charges in Eq. (50).

Consider a general Hamiltonian of a 2D Dirac point,

$$H = k_x \gamma_x + k_y \gamma_y, \quad (52)$$

where  $\gamma_i$ 's are  $\gamma$  matrices. The symmetries  $C_2$  and  $\Gamma$  imply

$$\{\Gamma, \gamma_{i=x,y}\} = 0, \quad \{C_2, \gamma_{i=x,y}\} = 0, \quad [\Gamma, C_2] = 0, \quad (53)$$

so they form the complex Clifford algebra

$$Cl_3 \otimes Cl_1 = \{\gamma_x, \gamma_y, \Gamma\} \otimes \{\gamma_x \gamma_y C_2\}, \quad (54)$$

as mentioned above. Then, if the Dirac point is unstable, there exists a Dirac mass term  $m\gamma_0$  consistent with the symmetries,

$$\{\Gamma, \gamma_0\} = 0, \quad [C_2, \gamma_0] = 0, \quad \{\gamma_{i=x,y}, \gamma_0\} = 0, \quad (55)$$

which modifies the Clifford algebra in Eq. (54) as

$$Cl_4 \otimes Cl_1 = \{\gamma_0, \gamma_x, \gamma_y, \Gamma\} \otimes \{\gamma_x \gamma_y C_2\}. \quad (56)$$

The modified algebra implies that the mass term  $\gamma_0$  behaves like an additional chiral operator  $\Gamma'$  that anticommutes with  $\Gamma$ . On the other hand, if the Dirac point is stable, no such an additional chiral operator exists. Therefore, the stability problem of the Dirac point reduces to the existence problem of an additional chiral operator [35,44].

The latter problem is solved as follows. By imposing chiral symmetry  $\Gamma$  on other generators, we have an extension of Clifford algebra

$$\begin{aligned} Cl_2 \otimes Cl_1 &= \{\gamma_x, \gamma_y\} \otimes \{\gamma_x \gamma_y C_2\} \\ \rightarrow Cl_3 \otimes Cl_1 &= \{\gamma_x, \gamma_y, \Gamma\} \otimes \{\gamma_x \gamma_y C_2\}, \end{aligned} \quad (57)$$

which defines the classifying space  $\mathcal{C}_0 \times \mathcal{C}_0$  in the K theory ( $\mathcal{C}_0 = \cup_{m,n} U(m+n)/(U(m) \times U(n))$ ; for details, see Refs. [35,44]). Because the classifying space consists of all possible matrix representations of  $\Gamma$  with other generators fixed, the zero-th homotopy group of the classifying space

$$\pi_0(\mathcal{C}_0 \times \mathcal{C}_0) = \mathbb{Z}^2 \quad (58)$$

measures topologically different chiral operators, specifying possible values for the topological number of  $\Gamma$ . Now we can show that if there is an additional chiral operator  $\Gamma'$ , then the topological number of  $\Gamma$  must be zero: Indeed, using  $\Gamma'$ , one can introduce the chiral operator  $\Gamma(t) = \Gamma \cos t + \Gamma' \sin t$  connecting  $\Gamma = \Gamma(0)$  and  $-\Gamma = \Gamma(\pi)$  continuously, which implies that  $\Gamma$  must be topologically trivial since topological numbers defined for chiral operators take opposite values for  $\Gamma$  and  $-\Gamma$  as we will see in an explicit way later [Eq. (61)]. Taking the contrapositive, we can also say that if the topological number of  $\Gamma$  is nontrivial, then no additional chiral operator exists. The last statement implies that the Dirac point is stable if the topological number of  $\Gamma$  is nontrivial. In other words, we can conclude that the topological charge protecting the Dirac point in Eq. (52) is given by Eq. (58), which coincides with Eq. (50) with  $N = 2$ .

The algebraic argument above can be intuitively understood by considering the specific Hamiltonian. Let us take the effective Hamiltonian of 2D half-flux square lattice,  $H = k_x \sigma_x \tau_z + k_y \sigma_y$  (i.e.,  $\gamma_x = \sigma_x \tau_z$ ,  $\gamma_y = \sigma_y$ ) with the twofold rotation symmetry  $C_2 = \sigma_z$ , and consider a possible generator  $\Gamma$  to form an algebra  $Cl_3 \otimes Cl_1 = \{\gamma_x, \gamma_y, \Gamma\} \otimes \{\gamma_x \gamma_y C_2\}$ . Since  $\Gamma$  anticommutes with  $\gamma_x$  and  $\gamma_y$  while commutes with  $\gamma_x \gamma_y C_2 = i \tau_z$ , it should be written as

$$\Gamma = \begin{pmatrix} s\sigma_z & 0 \\ 0 & s'\sigma_z \end{pmatrix}, \quad (59)$$

where the first and the second blocks correspond to  $\tau_z = \pm 1$ , respectively, and  $s, s' = \pm 1$ . Since  $\tau_z = \pm 1$  are decoupled, the sectors having different  $(s, s')$  cannot be connected by a continuous transformation, and thus they are topologically all distinct.

If we generally consider the matrix  $\tau_z$  with larger dimension such as  $\tau_z = \text{diag}(1, 1, \dots, -1, -1, \dots)$ , the possible expression for  $\Gamma$  is

$$\Gamma = \begin{pmatrix} \sigma_z \otimes A & 0 \\ 0 & \sigma_z \otimes A' \end{pmatrix}, \quad (60)$$

where the first and the second blocks in  $\Gamma$  correspond to  $\tau_z = \pm 1$ , respectively. Since we have  $\Gamma^2 = 1$ , eigenvalues of  $A$  and  $A'$  are either  $+1$  or  $-1$ . The topologically distinct phases are labeled by two integers,

$$(s, s') = (\text{tr}A, \text{tr}A'), \quad (61)$$

and this is  $\mathbb{Z}^2$  in Eq. (58). The winding number is given by  $\nu_W = s - s'$ , and the topological index of  $C_2 = +1$  sector (i.e., the difference between the numbers of the bases belonging to  $\Gamma = +1$  and  $-1$  in the  $C_2 = +1$  sector) is  $\nu_{\text{even}} = s + s'$ . So the space spanned by  $(s, s')$  is equivalent to that by  $(\nu_W, \nu_{\text{even}})$ .

### B. Class AIII with $C_3 R_z$ in 3D

We study the chiral-symmetric Dirac points with  $C_3 R_z$  symmetry (a combination of a threefold rotation in the  $x$ - $y$  plane and a reflection along the  $z$  axis) in a 3D Brillouin zone, for which we have discussed an example in the stacked honeycomb lattice model in Sec. VI. We write  $g = C_3 R_z$  and assume the commutation relation  $[g, \Gamma] = 0$ .

We consider a Dirac point located at the  $C_3 R_z$ -symmetric point and assume that the energy band is gapped in the vicinity

of the Dirac point, except for the Dirac point itself. At the Dirac point, we can define the six topological numbers  $\nu_{\pm 1}, \nu_{\pm\omega}, \nu_{\pm\omega^2}$  as we have seen in Sec. VI, but they are not completely independent. Since  $g^4 = C_3$  and  $g^3 = R_z$ , the  $C_3 R_z$  symmetry is always accompanied by the individual symmetries  $C_3$  and  $R_z$ . All the points on the  $k_z$  axis are fixed in  $C_3$ , and in order to have a band gap at these momenta (except for the Dirac point), all the indices for sectors  $C_3 = 1, \omega, \omega^2$  should be zero,

$$\nu_1 + \nu_{-1} = \nu_\omega + \nu_{-\omega} = \nu_{\omega^2} + \nu_{-\omega^2} = 0. \quad (62)$$

Here note that sectors  $g = \pm 1, \pm\omega, \pm\omega^2$  belong to those  $C_3 = 1, \omega, \omega^2$ , respectively. Similarly, since the  $k_x$ - $k_y$  plane is fixed in  $R_z$ , we have the following requirement:

$$\nu_1 + \nu_\omega + \nu_{\omega^2} = \nu_{-1} + \nu_{-\omega} + \nu_{-\omega^2} = 0, \quad (63)$$

in order to avoid a gap closing plane. Due to these constraints, we are left with only two independent indices, for example,  $\nu_1, \nu_\omega$ . We can also define a winding number on the  $R_z$ -symmetric plane. Let us perform the block diagonalization with respect to  $R_z = \pm 1$  on the  $R_z$ -symmetric plane. Then the  $R_z = +1$  sector is viewed as a 2D system class AIII+ $C_3$ , and we can define a winding number  $\nu_{W+}$  [Eq. (46)] for  $S^1$  surrounding the Dirac point. Similarly, we can also define  $\nu_{W-}$  for the  $R_z = -1$  sector. However, the total winding number  $\nu_W = \nu_{W+} + \nu_{W-}$  should vanish because a circle  $S^1$  defining the total winding number can be freely deformed in the 3D space so it is contractible without touching the Dirac point. Consequently, independent topological charges assigned to the Dirac point in the present case are a set of a winding number  $\nu_{W+}$  and two topological indices  $\nu_1, \nu_\omega$ ,

$$(\nu_{W+}, \nu_1, \nu_\omega) \in \mathbb{Z}^3. \quad (64)$$

For the Dirac point at  $K$  in the stacked honeycomb lattice model in Sec. VI, Eq. (44) leads to  $(\nu_{\pm 1}, \nu_{\pm\omega}, \nu_{\pm\omega^2}) = (\pm 1, \mp 1, 0)$ , which is consistent with the constraints Eqs. (62) and (63). The winding numbers  $\nu_{W\pm}$  can be evaluated using the effective Hamiltonian Eq. (43) as follows. On the  $R_z$ -symmetric plane ( $k_z = \pi/(2c)$ ), the Hamiltonian is expressed as

$$H = k_x \sigma_x \tau_z + k_y \sigma_y, \quad (65)$$

with  $R_z = \rho_z$  and  $\Gamma = \sigma_z \rho_z$ . It takes the same form in both the  $R_z = \pm 1$  sectors, but the chiral operator has an opposite sign, i.e.,  $\Gamma = \pm \sigma_z$ , leading to  $\nu_{W\pm} = \pm 1$  for the  $K$  point ( $\tau_z = +1$ ). Since  $\nu_{W\pm}$  is nonzero, nontrivial indices  $\nu_{a_i}$  are not necessary for the topological protection of the Dirac point in this particular example. However, if we consider a  $C_3 R_z$ -symmetric superlattice where the  $K$  and  $K'$  points are folded onto the same  $\Gamma$  point, as in the case of the 2D honeycomb lattice in Sec. III, the winding number around the Dirac point becomes zero while other indices  $\nu_{a_i}$  are still nonzero. There, the gaplessness at the Dirac point is solely guaranteed by nontrivial indices  $\nu_{a_i}$ .

### C. Class AIII with $C_2 R_z$ in 3D

Finally, we study the chiral-symmetric Dirac points with the inversion symmetry  $P = C_2 R_z$  in 3D. Here we consider two different cases, (i) where we have  $C_2$  and  $R_z$  symmetries individually and (ii) where we only have  $P$  but not  $C_2$  or  $R_z$ .

First, we consider case (i). The half-flux cubic lattice model argued in Sec. VI belongs to this case. We assume  $[C_2, R_z] = [C_2, \Gamma] = [R_z, \Gamma] = 0$ . At the inversion-symmetric point, we can define the four topological indices  $\nu_{++}, \nu_{+-}, \nu_{-+}, \nu_{--}$  for the sectors labeled by the eigenvalues of  $(C_2, R_z)$ . To avoid the band gap closing on the  $C_2$ -symmetric axis,

$$\nu_{++} + \nu_{+-} = \nu_{-+} + \nu_{--} = 0. \quad (66)$$

To gap out the  $R_z$ -symmetric plane, similarly, we require

$$\nu_{++} + \nu_{-+} = \nu_{+-} + \nu_{--} = 0. \quad (67)$$

Therefore  $(\nu_{++}, \nu_{+-}, \nu_{-+}, \nu_{--})$  is expressed by a single integer  $s$  as  $(s, -s, -s, s)$ . In Sec. VI, we defined the topological indices  $(\nu_{\text{even}}, \nu_{\text{odd}})$  for the sectors labeled by  $P = C_2 R_z$ , and they are related to the present indices by  $\nu_{\text{even}} = \nu_{++} + \nu_{--} = 2s$  and  $\nu_{\text{odd}} = \nu_{+-} + \nu_{-+} = -2s$ .

Similarly to the  $C_3 R_z$  case in the previous subsection, we can define the winding numbers  $\nu_{W\pm}$  for the  $R_z = \pm 1$  sector, respectively. The total winding number  $\nu_W = \nu_{W+} + \nu_{W-}$  vanishes again for the same reason. Therefore, independent topological charges assigned to a Dirac point are

$$(\nu_{W+}, \nu_{++}) \in \mathbb{Z}^2. \quad (68)$$

In case (ii), we can define the topological indices  $\nu_{\text{even}}, \nu_{\text{odd}}$  for the sectors labeled by the eigenvalues of the inversion  $P$  (where  $[P, \Gamma]$  is assumed). The summation  $\nu_{\text{even}} + \nu_{\text{odd}} = \text{tr } \Gamma$  should vanish, otherwise the band gap closes everywhere in  $k$  space. Unlike in case (i), we do not have the winding numbers  $\nu_{W\pm}$  since  $R_z$  symmetry is absent and thus we do not have a 2D subspace invariant under the symmetry operation. As a result, the Dirac point is characterized only by a single topological number,

$$\nu_{\text{even}} \in \mathbb{Z}. \quad (69)$$

Because  $C_2$  and  $R_z$  are both order-two operators, we can also derive the same conclusion from the analysis using Clifford algebra. Let us consider a 3D Dirac point,

$$H = k_x \gamma_x + k_y \gamma_y + k_z \gamma_z, \quad (70)$$

and explore whether a mass term  $m\gamma_0$  is allowed by imposed symmetries.

In case (i), we have three symmetries: chiral symmetry  $\Gamma$ , twofold rotation in the  $x$ - $y$  plane  $C_2$ , and reflection symmetry along the  $z$  direction  $R_z$ . The symmetry operators satisfy the following algebraic relations with the  $\gamma$  matrices:

$$\begin{aligned} \{\gamma_{i=0,x,y,z}, \Gamma\} &= 0, \\ [\gamma_{i=0,z}, C_2] = \{\gamma_{i=x,y}, C_2\} &= 0, \\ [\gamma_{i=0,x,y}, R_z] = \{\gamma_z, R_z\} &= 0, \end{aligned} \quad (71)$$

with the commutation relations with each other as follows:

$$[R_z, C_2] = [C_2, \Gamma] = [R_z, \Gamma] = 0. \quad (72)$$

Then we can construct a Clifford algebra from these relations as

$$Cl_6 \otimes Cl_1 = \{\gamma_0, \gamma_x, \gamma_y, \gamma_z, \gamma_z R_z, \Gamma\} \otimes \{\gamma_x \gamma_y C_2\}. \quad (73)$$

In a similar way as in Sec. VII A, the mass term  $\gamma_0$  can be considered an additional chiral operator  $\Gamma'$ , so if the

topological number of  $\Gamma$  is nonzero, then the Dirac point is stable. From an extension of Clifford algebra which is obtained by adding  $\Gamma$  to other generators,

$$\begin{aligned} Cl_4 \otimes Cl_1 &= \{\gamma_x, \gamma_y, \gamma_z, \gamma_z R_z\} \otimes \{\gamma_x \gamma_y C_2\} \\ \rightarrow Cl_5 \otimes Cl_1 &= \{\gamma_x, \gamma_y, \gamma_z, \gamma_z R_z, \Gamma\} \otimes \{\gamma_x \gamma_y C_2\}, \end{aligned} \quad (74)$$

we identify the relevant classifying space as  $\mathcal{C}_0 \times \mathcal{C}_0$ , and then the relevant topological number is evaluated as the zero-th homotopy,

$$\pi_0(\mathcal{C}_0 \times \mathcal{C}_0) = \mathbb{Z}^2, \quad (75)$$

which coincides with Eq. (68).

In case (ii), the additional symmetry is only an inversion  $P = C_2 R_z$ . The algebraic relations for  $P$  read as follows:

$$[\gamma_0, P] = \{\gamma_{i=x,y,z}, P\} = 0, \quad [P, \Gamma] = 0, \quad (76)$$

which form the Clifford algebra,

$$Cl_6 = \{\gamma_0, \gamma_x, \gamma_y, \gamma_z, \gamma_x \gamma_y \gamma_z P, \Gamma\}. \quad (77)$$

The existence condition for the mass term  $\gamma_0$  is obtained from the extension problem

$$\begin{aligned} Cl_4 &= \{\gamma_x, \gamma_y, \gamma_z, \gamma_x \gamma_y \gamma_z P\} \\ \rightarrow Cl_5 &= \{\gamma_x, \gamma_y, \gamma_z, \gamma_x \gamma_y \gamma_z P, \Gamma\}, \end{aligned} \quad (78)$$

which gives the classifying space as  $\mathcal{C}_0$ , and thus the topological charge protecting the Dirac point is given by

$$\pi_0(\mathcal{C}_0) = \mathbb{Z}. \quad (79)$$

This result reproduces Eq. (69).

## VIII. CONCLUSION

In this paper, we show that the coexistence of chiral symmetry and the spatial symmetry can stabilize zero-energy modes, even when the chiral symmetry alone does not ensure their stability. We present general arguments for the stability and we identify the associated topological numbers. The validity of our arguments are demonstrated for the Dirac points in two dimensions with a variety of spatial symmetries. We also illustrate that Dirac semimetals in three dimensions are possible in the presence of coexisting spatial symmetries. In the last part, we list and classify independent topological invariants associated with a given Dirac point. We find that the set of topological numbers found here gives a complete minimal set of quantum numbers allowed by the algebraic constraint in the case of order-two symmetries.

## ACKNOWLEDGMENTS

The authors acknowledge C. Hotta, K. Asano, and K. Shiozaki for useful discussions. This project was funded by JSPS Grants-in-Aid for Scientific Research [Grants No. 24740193 and No. 25107005 (M.K.), No. 24840047 (T.M.), and No. 22103005 and No. 25287085 (M.S.)].

- [1] X. G. Wen and A. Zee, *Nucl. Phys. B* **316**, 641 (1989).
- [2] A. P. Schnyder, S. Ryu, A. Furusaki, and A. W. W. Ludwig, *Phys. Rev. B* **78**, 195125 (2008).
- [3] A. Kitaev, *AIP Conf. Proc.* **1134**, 22 (2009).
- [4] S. Ryu and Y. Hatsugai, *Phys. Rev. Lett.* **89**, 077002 (2002).
- [5] S. Ryu, A. P. Schnyder, A. Furusaki, and A. W. Ludwig, *New J. Phys.* **12**, 065010 (2010).
- [6] J. C. Y. Teo and C. L. Kane, *Phys. Rev. B* **82**, 115120 (2010).
- [7] M. Sato, Y. Tanaka, K. Yada, and T. Yokoyama, *Phys. Rev. B* **83**, 224511 (2011).
- [8] L. Fu, *Phys. Rev. Lett.* **106**, 106802 (2011).
- [9] T. L. Hughes, E. Prodan, and B. A. Bernevig, *Phys. Rev. B* **83**, 245132 (2011).
- [10] A. M. Turner, Y. Zhang, and A. Vishwanath, *Phys. Rev. B* **82**, 241102(R) (2010).
- [11] T. H. Hsieh, H. Lin, J. Liu, W. Duan, A. Bansil, and L. Fu, *Nat. Commun.* **3**, 982 (2012).
- [12] R.-J. Slager, A. Mesaros, V. Juricic, and J. Zaanen, *Nat. Phys.* **9**, 98 (2013).
- [13] I. C. Fulga, B. van Heck, J. M. Edge, and A. R. Akhmerov, *Phys. Rev. B* **89**, 155424 (2014).
- [14] J. C. Y. Teo and T. L. Hughes, *Phys. Rev. Lett.* **111**, 047006 (2013).
- [15] Y. Ueno, A. Yamakage, Y. Tanaka, and M. Sato, *Phys. Rev. Lett.* **111**, 087002 (2013).
- [16] C.-K. Chiu, H. Yao, and S. Ryu, *Phys. Rev. B* **88**, 075142 (2013).
- [17] F. Zhang, C. L. Kane, and E. J. Mele, *Phys. Rev. Lett.* **111**, 056403 (2013).
- [18] S.-Y. Xu, C. Liu, N. Alidoust, M. Neupane, D. Qian, I. Belopolski, J. D. Denlinger, Y. J. Wang, H. Lin, L. A. Wray, B. Landolt, J. H. Slomski, J. H. Dil, A. Marcinkova, E. Morosan, Q. Gibson, R. Sankar, F. C. Chou, R. J. Cava, A. Bansil, and M. Z. Hasan, *Nat. Commun.* **3**, 1192 (2012).
- [19] Y. Tanaka, Z. Ren, T. Sato, K. Nakayama, S. Souma, T. Takahashi, K. Segawa, and Y. Ando, *Nat. Phys.* **8**, 800 (2012).
- [20] P. Dziawa, B. J. Kowalski, K. Dybko, R. Buczko, A. Szczerbakow, M. Szot, E. Łusakowska, T. Balasubramanian, B. M. Wojek, M. Berntsen, O. Tjernberg, and T. Story, *Nat. Mater.* **11**, 1023 (2012).
- [21] M. Z. Hasan and C. L. Kane, *Rev. Mod. Phys.* **82**, 3045 (2010).
- [22] X.-L. Qi and S.-C. Zhang, *Rev. Mod. Phys.* **83**, 1057 (2011).
- [23] S. Murakami, *New J. Phys.* **9**, 356 (2007).
- [24] X. Wan, A. M. Turner, A. Vishwanath, and S. Y. Savrasov, *Phys. Rev. B* **83**, 205101 (2011).
- [25] A. A. Burkov and L. Balents, *Phys. Rev. Lett.* **107**, 127205 (2011).
- [26] S. M. Young, S. Zaheer, J. C. Y. Teo, C. L. Kane, E. J. Mele, and A. M. Rappe, *Phys. Rev. Lett.* **108**, 140405 (2012).
- [27] Z. Wang, Y. Sun, X.-Q. Chen, C. Franchini, G. Xu, H. Weng, X. Dai, and Z. Fang, *Phys. Rev. B* **85**, 195320 (2012).
- [28] Z. Wang, H. Weng, Q. Wu, X. Dai, and Z. Fang, *Phys. Rev. B* **88**, 125427 (2013).
- [29] B.-J. Yang and N. Nagaosa, *Nat. Commun.* **5**, 4898 (2014).
- [30] M. Neupane, S.-Y. Xu, R. Sankar, N. Alidoust, G. Bian, C. Liu, I. Belopolski, T.-R. Chang, H.-T. Jeng, H. Lin, A. Bansil, F. Chou, and M. Z. Hasan, *Nat. Commun.* **5**, 3786 (2014).
- [31] S. Borisenko, Q. Gibson, D. Evtushinsky, V. Zabolotnyy, B. Büchner, and R. J. Cava, *Phys. Rev. Lett.* **113**, 027603 (2014).
- [32] Z. K. Liu, B. Zhou, Y. Zhang, Z. J. Wang, H. M. Weng, D. Prabhakaran, S.-K. Mo, Z. X. Shen, Z. Fang, X. Dai, Z. Hussain, and Y. L. Chen, *Science* **343**, 864 (2014).
- [33] C. Herring, *Phys. Rev.* **52**, 365 (1937).
- [34] K. Asano and C. Hotta, *Phys. Rev. B* **83**, 245125 (2011).
- [35] T. Morimoto and A. Furusaki, *Phys. Rev. B* **88**, 125129 (2013).
- [36] K. Shiozaki and M. Sato, *arXiv:1403.3331*.
- [37] S. Kobayashi, K. Shiozaki, Y. Tanaka, and M. Sato, *Phys. Rev. B* **90**, 024516 (2014).
- [38] J. McClure, *Phys. Rev.* **104**, 666 (1956).
- [39] T. Ando, *J. Phys. Soc. Jpn.* **74**, 777 (2005).
- [40] M. S. Dresselhaus and G. Dresselhaus, *Adv. Phys.* **51**, 1 (2002).
- [41] I. Affleck and J. B. Marston, *Phys. Rev. B* **37**, 3774 (1988).
- [42] P. Hořava, *Phys. Rev. Lett.* **95**, 016405 (2005).
- [43] Y. X. Zhao and Z. D. Wang, *Phys. Rev. Lett.* **110**, 240404 (2013).
- [44] T. Morimoto and A. Furusaki, *Phys. Rev. B* **89**, 235127 (2014).